Comparison of noninvasive fluorescent and bioluminescent small animal optical imaging

Garry Choy[1], Sarah O'Connor[1], Felix E. Diehn[2], Nick Costouros[1], H. Richard Alexander[1], Peter Choyke[2], and Steven K. Libutti[1]

BioTechniques 35:1022-1030 (November 2003)

Optical imaging is a modality that is cost-effective, rapid, easy to use, and can be readily applied to studying disease processes and biology in vivo. For this study, we used a green fluorescent protein (GFP)- and luciferase-expressing mouse tumor model to compare and contrast the quantitative and qualitative capabilities of a fluorescent reporter gene (GFP) and a bioluminescent reporter gene (luciferase). We describe the relationship between tumor volume, tumor mass, and bioluminescent/fluorescent intensity for both GFP and luciferase. Bioluminescent luciferase imaging was shown to be more sensitive than fluorescent GFP imaging. Luciferase-expressing tumors were detected as early as 1 day after tumor cell inoculation, whereas GFP-expressing tumors were not detected until 7 days later. Both bioluminescent and fluorescent intensity correlated significantly and linearly with tumor volume and tumor weight, as measured by caliper. Compared to bioluminescent imaging, fluorescent imaging does not require the injection of a substrate and may be appropriate for applications where sensitivity is not as critical. Knowing the relative strengths of each imaging modality will be important in guiding the decision to use fluorescence or bioluminescence.

INTRODUCTION

Recently, there has been increasing interest and efforts devoted to developing methods for whole-body imaging in mice. The currently available imaging technologies such as magnetic resonance imaging (MRI), computed tomography (CT), positron emission tomography (PET), and single photon emission computed tomographic (SPECT) offer deep tissue penetration and high spatial resolution. However, compared to noninvasive small animal optical imaging, these techniques are very costly and time-consuming to implement. Optical imaging is a modality that is cost-effective, rapid, easy to use, and can be readily applied to studying disease processes and biology in vivo.

Two commonly used reporter genes, green fluorescent protein (GFP) and luciferase, have been extensively used in vivo and in vitro. GFP, originally cloned from the jellyfish *Aequorea victoria*, has also been used extensively to study subcellular processes such as gene expression and protein localization (1–4). Typical of fluorescent imaging, acquisition of GFP signal relies on excitation by an external light source. Bioluminescence imaging, on the other hand, is based on the endogenous production of light by the expression of the enzyme luciferase. This enzyme, found in fireflies and other bioluminescent organisms, produces light upon reacting with the substrate luciferin in the presence of oxygen and ATP. Like GFP, luciferase has been used extensively in vitro to study cellular processes (5,6). In small animal imaging, GFP and luciferase have both been employed to study transgene expression, tumor growth/treatment/metastasis, and infectious disease processes (7–18). Despite these similarities in their applications, bioluminescent imaging differs considerably from fluorescent imaging.

Since bioluminescent imaging does not require an excitation light source, there is extremely low background, which is often caused by autofluorescence. Hence, bioluminescent imaging enables the imaging of processes that produce minimal signal, such as in the case of lymphocyte trafficking in vivo or the detection of a small number of cancer cells in vivo (19–23). Furthermore, GFP fluorescent images can be acquired in real-time in the millisecond range, while bioluminescent images are acquired in the minute timescale.

GFP- and luciferase-based imaging techniques both differ in the type of information obtained and in implementation. As a result, fluorescent and bioluminescent imaging can be applied differently in vivo for specific scientific investigations. Considering the unique abilities and unique applications of either GFP or luciferase, experiments that compare these two imaging techniques qualitatively and quantitatively have not yet been described. In this study, we use a GFP- and luciferase-expressing mouse tumor model to compare the two optical imaging techniques. We compare the sensitivity of both techniques in detecting tumor lesions as well as their ability to quantitatively describe the relationship between tumor volume, tumor mass, and bioluminescent/fluorescent intensity.

[1]National Cancer Institute, NIH, Bethesda and [2]Warren G. Magnuson Clinical Center, NIH, Bethesda, MD, USA

MATERIALS AND METHODS

Retroviral GFP and Luciferase Transduction

Vectors pCLNC-GFP, pMD.G, and cell line 293GP were obtained from P. Robbins, National Cancer Institute (NCI), Bethesda, MD. Vector pCLNC-LUC, containing the (firefly) luciferase gene, was constructed in our laboratory and is based on the pCLNCX retroviral vector system (24). Vector pCLNC-GFP contains the GFP gene and is based on the pCLNCX retroviral vector system (24). Pseudotyped retroviral particles were generated as previously described (25). In brief, 293GP cells were stably transfected with retroviral *gag* and *pol* elements. The pMD.G vector contains the G protein gene from vesicular stomatitis virus. The 293GP cells were then cotransfected with the pMD.G and pCLNC-GFP vectors. MC38 murine colon adenocarcinoma cells (Surgery Branch, NCI) were transduced with retroviral supernatant in the presence of hexadimethrine bromide (8 µg/mL; Sigma, St. Louis, MO, USA) and selected in G418 (400 µg/mL; Invitrogen, Carlsbad, CA, USA). Expression of GFP was assessed by fluorescence microscopy. Expression of luciferase in each clone was assessed by a commercially available Luciferase Assay System (Promega, Madison, WI, USA). The in vitro growth rate of the MC38-GFP cell line was similar to that of the parental line, and the expression of GFP was stable in vitro even in the absence of selection agents (data not shown).

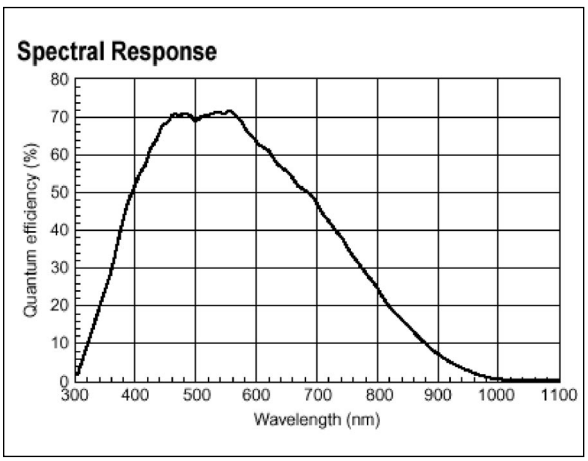

Figure 1. Spectral sensitivity of ORCA 2-ER charge-coupled device (CCD) camera used in this study.

Whole-Body Optical Imaging System

Imaging was conducted using an ORCA 2-ER charge-coupled device (CCD) camera (Hamamatsu Photonics KK, Hamamatsu, Japan) fitted with a c-mount 2/3″ format, 12.5–75 mm, f1.8 lens (Toyo, Irvine, CA, USA) attached to a custom-made light-tight imaging chamber (Microscopic Services, Rockville, MD, USA). The detector uses an ER-150 (Hamamatsu Photonics KK) CCD progressive scan interline chip with microlens and is cooled by Peltier cooling/forced-air cooling with hermetic sealing. The spectral sensitivity of the detector is illustrated in Figure 1. Before all imaging, mice were shaved to remove fur. Mice were then anesthetized with 7 to 8 mg ketamine/xylazine injected intraperitoneally (i.p.). For fluorescent imaging, a 150 W light source (Schott-Fostec, New York, NY, USA) and a GFP filter set [excitation filter (HQ470, 40×), barrier filter (OG515); Chroma, Brattleboro, VT, USA] were used. An integration time of 200–300 ms was used for GFP signal acquisition. For bioluminescent imaging, the GFP barrier filter was removed, and the light source was turned off. Five minutes prior to imaging, the substrate luciferin (Biotium, Hayward, CA, USA) suspended in phosphate-buffered saline (PBS) (20 mg/mL) was injected i.p. at a dose of 100 mg/kg. An integration time of 10 min was used for bioluminescent image acquisition. All images were transferred to a Power Mac® G4 computer and were analyzed by Openlab 3.1 software (Improvision, Lexington, MA, USA).

Tumor Formation and Implantation in Animals

MC38-GFP or MC38-LUC cell lines were cultured in Dulbecco's modified Eagle's medium (DMEM), 10% fetal calf serum, 100 U/mL penicillin, 100 µg/mL streptomycin, 50 µg/mL gentamicin, 0.5 µg/mL fungizone, and 4 mM glutamine (Biofluids, Rockville, MD USA). Seven-week-old female B57BL/6 mice were shaved and injected subcutaneously (s.c.) with 1×10^6 cells suspended in PBS on their flank. At indicated time points, the length and width of tumors were measured by calipers. Tumor volumes were calculated according to the formula:

$$\text{volume} = 0.52 \times \text{length} \times \text{width}^2$$

(0.52 is the constant used to calculate volume for an ellipsoid). All animal experiments were conducted under protocols approved by the National Institutes of Health (NIH) Animal Care and Use Committee (Bethesda, MD, USA).

Western Blot Analysis

To assess expression levels of GFP and luciferase, Western blot analysis was performed on both excised tumors (5 days postinjection) and cell lines. Cultured cells were lysed using radioimmunoprecipitation assay (RIPA) buffer (26). Specifically, approximately 1×10^7 of MC38-GFP and 1×10^7 MC38-LUC were lysed for protein extraction yielding comparable concentrations of protein in lysate. Excised tumors were homogenized using FastPrep® FP120 (Thermo Savant, Holbrook, NY, USA) in RIPA buffer. Extracts of cultured cells and excised tumors were then loaded (30 µg/lane). Lysates were then resolved by sodium dodecyl sulfate polyacrylamide gel electrophoresis (SDS-PAGE) and transferred to nitrocellulose membranes. For MC38-GFP cells and tumors, a primary antibody to GFP was used (AbCam, Cambridge, UK). For MC38-LUC cells and tumors, a primary antibody to firefly luciferase was used (AbCam). Secondary antibodies (Amersham Biosciences, Piscataway, NJ, USA) were horseradish peroxidase-conjugated, and detection was performed using the ECL™ chemiluminescence kit (Amersham Biosciences). To assess expression levels, blots were digitized and analyzed by software (NIH Image, Bethesda, MD, USA).

Animal Sacrifice

MC38-GFP and MC38-Luc tumors were harvested and weighed immediately after the mice were sacrificed at the conclusion of the experiments. No

desiccation of tumor was performed prior to measurements.

Statistical Methods

Microsoft® Excel® was used to perform all statistical analysis. All data represent mean values ± standard errors ($\bar{X} \pm$ SEM).

RESULTS AND DISCUSSION

A murine colon adenocarcinoma line (MC38) was successfully engineered to stably express either GFP or luciferase by retroviral transduction, and the highest expressing clones were selected for in vivo study. MC38-GFP and MC38-LUC murine colon adenocarcinoma xenografts were implanted s.c. into the right flanks of mice. Tumor burden over time was followed with volume measurements by caliper and noninvasive fluorescent and bioluminescent imaging (Figure 2, A–D). Bioluminescent luciferase imaging was shown to be more sensitive than fluorescent GFP imaging. Luciferase-expressing (MC38-LUC) tumors were detected as early as 1 day (Figure 2B) after tumor cell inoculation, whereas GFP-expressing (MC38-GFP) tumors were not detected until 7 days later. For both tumor types, caliper measurements could be performed by day 5 postinjection (Figure 2, A and C).

For both types of imaging, bioluminescent and fluorescent intensity correlated significantly and linearly with tumor volume, as measured by caliper (Figure 3, A and B). For GFP fluorescent imaging, a slightly stronger correlation was found between fluorescent intensity and tumor weight (Figure 3E; $R^2 = 0.83$) than between tumor volume and weight (Figure 3C; $R^2 = 0.80$). A significantly stronger correlation was found between bioluminescent intensity and tumor weight (Figure 3F; $R^2 = 0.93$) than between volume and weight (Figure 3D; $R^2 = 0.82$). Each group initially consisted of ten mice, and seven to eight per group survived through the course of the experiments.

Western blot analysis was also performed to confirm in vitro and in vivo expression of both GFP and luciferase (Figure 4). Results demonstrate that there is stable expression of GFP and luciferase in cell culture as well as in tumors that excised 5 days postinjection. Specifically in the cultured cell lines, expression level of GFP was similar to that of luciferase (relative expression of GFP/luciferase = 1.3). Because the mechanism of light production for both GFP and luciferase are completely different, it is important to note that even equal levels of GFP and luciferase protein do not necessarily guarantee the same level of light production.

Although both whole-mouse fluorescent and bioluminescent imaging has proven useful, the direct comparison of these two techniques has not yet been described. Here, we have attempted to use GFP- and luciferase-expressing murine colon adenocarcinomas to characterize both qualitative and quantitative abilities of these two types of optical imaging techniques.

We have demonstrated that serial tumor volume measurements by caliper closely matched photon count (bioluminescence) and fluorescent intensity (Figure 3). A significant correlation ($R^2 = 0.99$) between tumor volume measurement and fluorescent intensity was found, which supports our previously published data (18). Bioluminescent imaging also correlated well to tumor volume measurements ($R^2 = 0.97$) (Figure 3, A and B). This experiment suggests that both GFP- and luciferase-based imaging techniques can be readily used to assess changes in tumor volume over time.

We also describe the quantitative relationships between tumor mass, tumor volume, and fluorescent intensity or photon count. On the last day of experiments, mice were euthanized and tumors

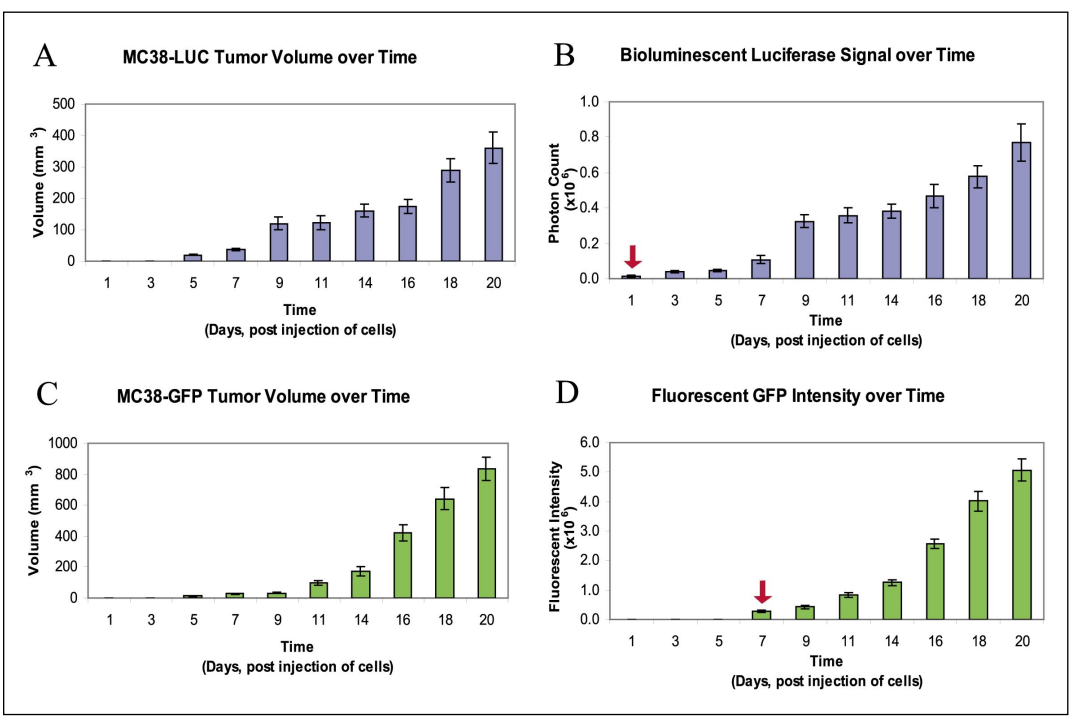

Figure 2. Serial measurements of tumor volume, fluorescence, and bioluminescence. MC38-LUC or MC38-GFP tumor cells were injected subcutaneously (s.c.) into the right flanks of C57/BL6 mice. Both tumor volume measurements by caliper and noninvasive whole-body optical imaging were performed every other day after injection. (A) Serial tumor volume measurements of MC38-LUC xenografts. (B) Bioluminescence over time. Red arrow indicates initial detection of signal. (C) Serial tumor volume measurements of MC38-GFP xenografts. (D) Fluorescence over time. Red arrow indicates initial detection of signal. $n = 7–10$ per group.

were weighed. We found that tumor weight and tumor volume correlated linearly for both GFP (R^2 = 0.80) and luciferase (R^2 = 0.82) imaging (Figure 3, C and D). However, the correlation between tumor weights and fluorescent intensity or photon count was slightly more robust for GFP and significantly more robust for luciferase than correlations with volume measurements. Interestingly, the correlation between tumor weight and imaging quantification was stronger (R^2 = 0.92) for luciferase than for GFP (R^2 = 0.83) (Figure 3, E and F). This suggests that bioluminescence may be a more sensitive method for estimating the true volume of viable cells in the tumor (assuming that true

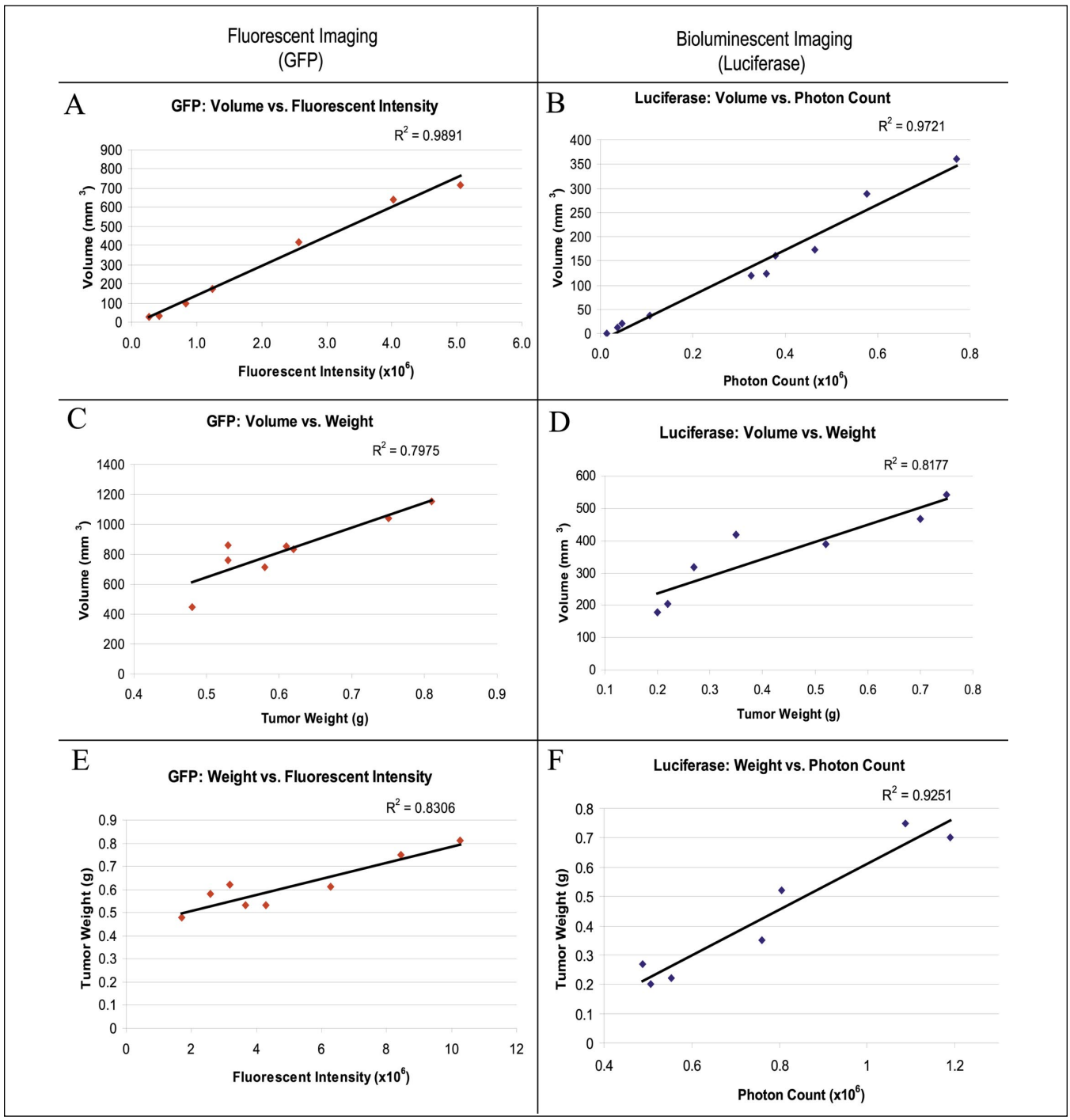

Figure 3. Correlations of tumor volume, tumor weight, fluorescent intensity, and photon counts. (A and B) Tumor volumes of MC38-GFP xenografts (A) and MC38-LUC xenografts (B) were correlated to fluorescent intensities on each experimental time point. (C–F) On day 20, mice were sacrificed and tumors were harvested and weighed. The MC38-GFP tumor weights were then correlated to tumor volume (C) and fluorescent intensity (E). The MC38-LUC tumor weights were correlated to tumor volume (D) and photon counts (F). n = 7–10 per group.

Table 1. Summary of Comparative Features of GFP-Based Fluorescent Imaging and Luciferase-Based Bioluminescent Imaging

	GFP	Luciferase
Signal-to-noise ratio	Low	High
Earliest tumor detection in experiment	Day 7	Day 1
No. of mice that can be imaged	Few (one mouse for our system; depends on excitation light source design)	Many (up to 10 mice demonstrated in our system)
Substrate	None	Luciferin
Volume vs. imaging correlation	0.99	0.97
Biomass vs. imaging correlation	0.81	0.93
Image acquisition time	Milliseconds (200–300 ms)	Minutes (10 min)
Special requirements	none	ATP plus oxygen required for sufficient light production

biomass is closely related to weight) than fluorescence.

Furthermore, bioluminescent imaging was able to detect tumors significantly earlier than fluorescent imaging. Luciferase-expressing tumors were detected as early as 1 day after injection of tumor cells, whereas GFP fluorescence was not detected until day 7 postinjection (Figure 3). This result highlights the high sensitivity and minimal background intrinsic to bioluminescent imaging. Background signal noise is minimal because there is virtually no endogenous bioluminescence from mammalian cells. However, GFP fluorescence is hampered by severe autofluorescence due to light reflection and light absorbance and scattering, thereby preventing the detection of low signals. Researchers are currently investigating and developing new technologies to address the problem of autofluorescence. For example, Levenson and colleagues have demonstrated that background in GFP fluorescence imaging can be eliminated using a novel method of spectral imaging (19).

Fluorescent and bioluminescent imaging modalities each offer distinct advantages that can be maximized, depending on the application. Features of both types of imaging are compared in Table 1. Certain types of experiments may deem luciferase-based imaging to be more appropriate. If one needs to detect low signals, luciferase-based imaging may be the better choice. For example, luciferase-based imaging has been used for studying lymphocyte tracking, in which the signal is extremely low (25). Because luciferase allows for the detection of low and high signals, bioluminescent imaging provides a wider dynamic range. Interestingly, longer wavelengths permit deeper tissue penetration in vivo. In contrast to an emission of 510 nm by GFP, the luciferase-luciferin reaction produces light that emits at a longer wavelength of approximately 600 nm, possibly enabling deeper tissue penetration. As a result, luciferase-based imaging may be useful in situations where one needs higher sensitivity, wider dynamic signal bandwidth, and deeper tissue penetration.

In other applications, GFP fluorescent imaging may be worth considering. GFP is extensively used in cell biology and in vitro assays for its strong signal and microscopic-level spatial resolution. If whole-body mouse imaging needs to be combined or followed by in vitro assays, GFP is a very viable option. The acquisition of the fluorescent GFP signal also does not require substrate injection, thereby minimizing the preparative procedures required, and i.p. injections may be prohibitive in certain types of experiments. Since luciferin is a relatively expensive substrate, GFP may also be more cost-effective.

However, if GFP is to be used, the issues of autofluorescence and lower sensitivity must be taken into account. To achieve greater depth of penetration and to minimize the problem of autofluorescence in GFP imaging, Hoffman et al. reported that steps such as skin flaps and endoscopic technology can be used (8). In other studies, CCD cameras have been attached to microscopes, which enable higher magnification to aid in the detection of small GFP-labeled tumors (20,21). Furthermore, the intensity of GFP signals can be very high and can therefore

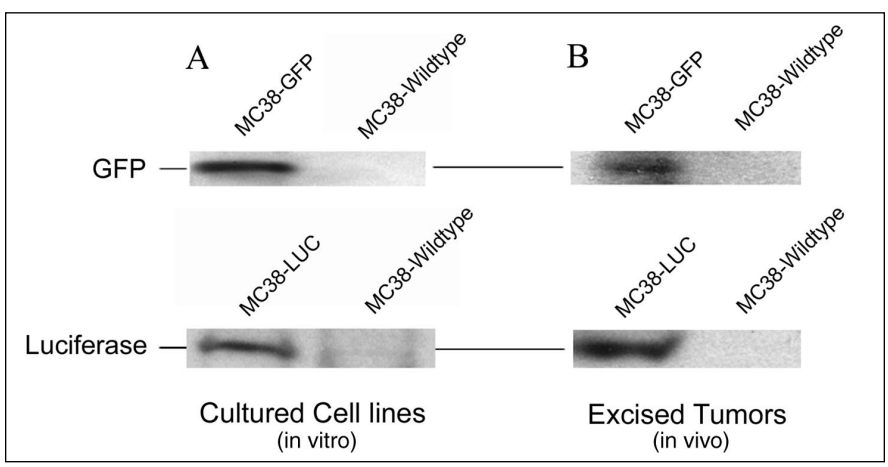

Figure 4. Western blot analysis of in vitro and in vivo green fluorescent protein (GFP) and luciferase expression. (A) Expression levels of GFP and luciferase protein from lysates of cells in culture. (B) Expression levels of GFP and luciferase protein from extracts of excised tumors that were resected 5 days postimplantation.

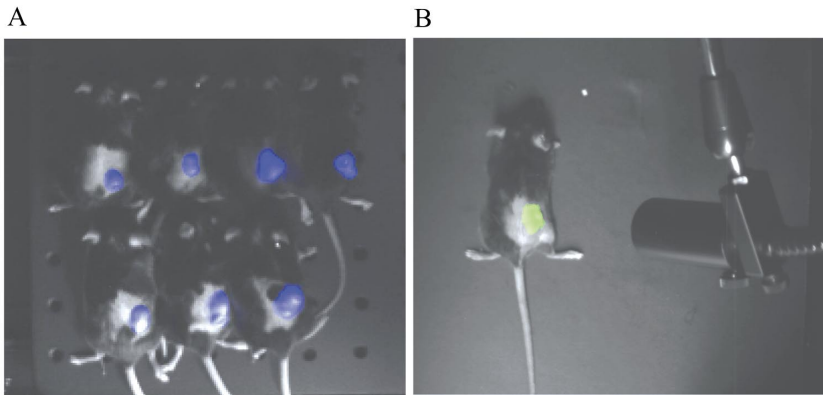

Figure 5. Comparison of the number of mice that can be imaged simultaneously via bioluminescent imaging and fluorescent imaging. (A) Sample image of bioluminescence imaging, in which many mice can be imaged at the same time. All mice need to be injected with the substrate luciferin prior to imaging, and no external light source is required. (B) GFP fluorescent imaging requires an external light source emitting at a specific wavelength of 510 nm. The excitation light source has an optimal center of intensity so only one tumor/mouse can be optimally imaged at any one time.

allow for extremely short image exposure times. As a result, CCD cameras can perform real-time imaging of GFP in nonanesthetized and active animals with implanted tumors (2).

Hardware design is also dependent on the type of imaging performed. Fluorescent imaging requires an external light source, whereas bioluminescent imaging does not. In bioluminescent imaging, light is emitted endogenously from the tissue due to the luciferase-luciferin chemical reaction. However, fluorescent mouse imaging can be limited by the design of the excitation light source. In our imaging system, there is only one excitation fiber-optic light source, which can only allow for imaging of one mouse at a time. As a result, the number of mice that can be imaged by fluorescence imaging depends on the design of the excitation light source. The scalability of both types of imaging is illustrated in Figure 5.

In addition to equipment for fluorescence imaging, the CCD is a key component of any optical imaging system that must be carefully chosen. Our imaging system configuring consists of a CCD camera that is sensitive to emission wavelengths for both GFP and luciferase. These technical specifications can be further optimized, as there are

numerous equipment types available on the market. In addition to high signal-to-noise ratios for the detector, high quantum efficiency over the emission wavelengths needs to be a primary criterion in hardware selection (27).

Cytotoxicity of both GFP and luciferase may also be a possible concern that should be considered by the investigator. Despite the extensive use of luciferase and GFP for in vitro studies, the potential toxicities of these reporters have yet to be fully investigated. For example, where some studies have documented the nontoxic nature of GFP, some studies have demonstrated that GFP may be toxic and that high protein levels may induce apoptosis (20,28). When excited for extended periods of time, GFP may also generate free radicals with potentially cytotoxic properties (29). Luciferase and its substrate, luciferin, have been reported to mainly exhibit low toxicity with no apparent effects on the health of animals (16,17,22,23). Because questions remain regarding the immunogenicity and toxicity of these reporters and also the substrate luciferin, this may be a potential avenue of future study.

Thus far, we have demonstrated the quantitative capabilities of both luciferase-based bioluminescent and GFP-based fluorescent in vivo imaging. Both GFP and luciferase, as reporter constructs, have been shown to harness distinct strengths that can be taken into consideration when choosing fluorescence or bioluminescence as the optical imaging modality for a particular experiment. Each technique has a role, and the two may be complementary.

ACKNOWLEDGMENTS

G.C. is a Howard Hughes Medical Institute-NIH Research Scholar.

REFERENCES

1. **Prasher, D.C. V.K. Eckenrode, W.W. Ward, F.G. Prendergast, and M.J. Cormier.** 1992. Primary structure of the *Aequorea victoria* green-fluorescent protein. Gene *111*:229-333.
2. **Subramanian, S. and F. Srienc.** 1996. Quantitative analysis of transient gene expression in mammalian cells using the green fluorescent protein. J. Biotechnol. *49*:137-151.
3. **Chalfie, M.** 1995. Green fluorescent protein. Photochem. Photobiol. *62*:651-656.
4. **Kain, S.R, M. Adams, A. Kondepudi, T.T. Yang, W.W. Ward, and P. Kitts.** 1995. Green fluorescent protein as a reporter of gene expression and protein localization. BioTechniques *19*:650-655.
5. **Hastings, J.W.** 1996. Chemistries and colors of bioluminescent reactions: a review. Gene *173*:5-11.
6. **Wood, K.V.** 1996. Marker proteins for gene expression. Curr. Opin. Biotech. *6*:50-80.
7. **Contag, C.H., D. Jenkins, P.R. Contag, and R.S. Negrin.** 2000. Use of reporter genes for optical measurements of neoplastic disease in vivo. Neoplasia *2*:41-52.
8. **Hoffman, R.M.** 2001. Visualization of GFP-expressing tumors and metastasis in vivo. BioTechniques *30*:1016-1024.
9. **Bouvet, M., J. Wang, S.R. Nardin, R. Nasirpour, M. Yang, E. Baranov, P. Jiang, A.R. Moossa, and R.M. Hoffman.** 2000. Real-time optical imaging of primary tumor growth and multiple metastatic events in a pancreatic cancer orthotopic model. Cancer Res. *62*:1534-1540.
10. **Hasegawa, S., M. Yang, T. Chishima, Y. Miyagi, H. Shimada, A.R. Moossa, and R.M. Hoffman.** 2001. In vivo tumor delivery of the green fluorescent protein gene to report future occurrence of metastasis. Cancer Gene Ther. *7*:1336-1340.
11. **Hoffman, R.M.** 2001. Visualization of GFP-expressing tumors and metastasis in vivo. BioTechniques *30*:1016-1024.
12. **Yang, M., E. Baranov, J.W. Wang, P. Jiang, X. Wang, F.X. Sun, M. Bouvet, A.R. Moossa, et al.** 2002. Direct external imaging of nascent cancer, tumor progression, angiogenesis, and metastasis on internal organs in the fluorescent orthotopic model. Proc. Natl. Acad. Sci. USA *99*:3824-3829.
13. **Zhao, M., E. Yang, E. Baranov, X. Wang, S. Penman, A.R. Moossa, and R.M. Hoffman.** 2001. Spatial-temporal imaging of bacterial infection and antibiotic response in intact animals. Proc. Natl. Acad. Sci. USA *98*:9814-9818.
14. **Rehemtulla, A., L.D. Stegman, S.J. Cardozo, S. Gupta, D.E. Hall, C.H. Contag, and B.D. Ross.** 2000. Rapid and quantitative assessment of cancer treatment response using in vivo bioluminescence imaging. Neoplasia *2*:491-495.
15. **Sweeney, T.J., V. Mailaender, A.A. Tucker, A.B. Olomu, W. Zhang, Y. Cao, R.S. Negrin, and C.H. Contag.** 1999. Visualizing the kinetics of tumor-cell clearance in living animals. Proc. Natl. Acad. Sci. USA *96*:12044-12049.
16. **Contag, C.H., P.R. Contag, J.L. Mullins, S.D. Spilman, D.K. Stevenson, and D.A. Benaron.** 1995. Photonic detection of bacterial pathogens in living hosts. Mol. Microbiol. *18*:593-603.
17. **Contag, C.H., S. Spilman, P.R. Contag, M. Oshiro, B. Eames, P. Dennery, D.K. Stevenson, and D.A. Benaron.** 1997. Visualizing gene expression in living animals using a bioluminescent reporter. Photochem. Photbiol. *66*:523-531.
18. **Diehn, F.E., N.G. Costouros, M.S. Miller, A.L. Feldman, H.R. Alexander, K.C.P. Li, and S.K. Libutti.** 2002. Noninvasive fluorescent imaging reliably estimates biomass in vivo. BioTechniques *33*:1250-1255.
19. **Levenson, R., M. Yang, and R.M. Hoffman.** 2003. Whole-body spectral imaging of fluorescently labeled orthotopic lung tumors in the live mouse. Proc. Am. Assoc. Cancer Res. *44*:776.
20. **Yang, M., E. Baranov, P. Jiang, F.X. Sun, X.M. Li, L. Li, S. Hasegawa, M. Bouvet, et al.** 2000. Whole-body optical imaging of green fluorescent protein-expressing tumors and metastases. Proc. Natl. Acad. Sci. USA *97*:1206-1211.
21. **Chaudhuri, T.R., J.M. Mountz, B.E. Rogers, E.E. Partridge, and K.R. Zinn.** 2001. Light-based imaging of green fluorescent protein-positive ovarian cancer xenografts during therapy. Gynecol. Oncol. *82*:581-589.
22. **Hardy, J., M. Edinger, M.H. Bachmann, R.S. Negrin, C.G. Fathman, and C.H. Contag.** 2001. Bioluminescence imaging of lymphocyte trafficking in vivo. Exp. Hematol. *29*:1353-1360.
23. **Edinger, M., T.J. Sweeney, A.A. Tucker, A.B. Olomu, R.S. Negrin, and C.H. Contag.** 1999. Noninvasive assessment of tumor cell proliferation in animal models. Neoplasia *1*:303-310.
24. **Naviaux, R.K., E. Costanzi, M. Haas, and I.M. Verma.** 1996. The pCL vector system: rapid production of helper-free, high-titer, recombinant retroviruses. J. Virol. *70*:5701-5705.
25. **Feldman, A.L., H.R. Alexander, S.M. Hewitt, D. Lorang, C.E. Thiruvathukal, E.M. Turner, and S.K. Libutti.** 2001. Effect of retroviral endostatin gene transfer on subcutaneous and intraperitoneal growth of murine tumors. J. Natl. Cancer Inst. *93*:1014-1020.
26. **Atadja, P., H. Wong, C. Veillette, and K. Riabowol.** 1995. Overexpression of cyclin D1 blocks proliferation of normal diploid fibroblasts. Exp. Cell Res. *217*:205-216.
27. **Rice, B.W., M.D. Cable, and M.B. Nelson.** 2001. In vivo imaging of light-emitting probes. J. Biomed. Optics *6*:432-440.
28. **Liu, H., M. Jan, C. Chou, P. Chen, and N. Ke.** 1999. Is green fluorescent protein toxic to the living cells? Biochem. Biophys. Res. Commun. *260*:712-717.
29. **Clontech**. 1996. Living Color GFP Application Notes. CLONTECH Laboratories, Palo Alto, CA.

Received 4 May 2003; accepted 2 September 2003.

Address correspondence to:

Steven K. Libutti
Surgery Branch, Center for Cancer Research
National Cancer Institute
10 Center Drive, Room 2B07
Bethesda, MD 20892, USA
e-mail: libuttis@mail.nih.gov